7th ECCOMAS Thematic Conference on Smart Structures and Materials
SMART 2015
Stefan Storm, Johannes Kirn

Towards the Industrial Application of Morphing Aircraft Wings - Development of the Actuation Kinematics of a Droop Nose

Stefan Storm [*], **Johannes Kirn** [†]

[*] Airbus Group Innovations (AGI)
Munich, Germany
Stefan.Storm@Airbus.com

[†] Airbus Group Innovations (AGI)
Munich, Germany
Johannes.Kirn@Airbus.com

Key words: Morphing, Adaptive aircraft, System design, Kinematics, Actuation systems, Laminar wing, Optimization tool.

Summary:

This paper describes the design process of a least complex actuation system capable of smoothly modifying an extensive flexible skin applied to a leading edge droop nose of laminar wings.

1 INTRODUCTION

The idea of morphing wings goes all the way back to the Wright brothers who used wing warping to control their flying machines at the end of 19th century. Since then many experimental and numerical studies showed the aerodynamic benefit of morphing wings in various application scenarios but until now, over one century after its first application, morphing is still not a state-of-the-art technology in civil transport aircraft. Some necessary steps towards the industrialization of morphing have been taken in the EU (FP7) project SARISTU (Smart Intelligent Aircraft Structures) [1].

The application case is a seamless and gapless leading edge droop nose (EADN) for a single aisle transport aircraft. As enabler for laminar wings the droop nose contributes to a 6% drag reduction and thus to positive implications on fuel consumption and required take-off fuel load [2][3]. The selected droop nose concept consists of a flexible skin being actuated by a composition of kinematics and actuators [4][5].

The actuation of the leading edge poses a huge challenge for the internal kinematics as it has to synergize with other functionalities like bird strike protection, de-icing, surface and lightning protection. The design of the kinematics is therefore a key element for the development of a droop nose. In this context this paper focuses on computational modeling as a design tool.

2 DEVELOPMENT OF THE ACTUATION KINEMATICS OF A DROOP NOSE

Work on an adaptive droop-nose kinematic actuation system started in the previous projects InHiD (LuVo IV) and SADE (EU-FP7) where the feasibility of such a system was demonstrated. In the project SADE (FP7) studies with different kind of actuation mechanism for smart leading edges were performed such as eccentric beam mechanism, horn concept, fluidic actuator concept, kinematic chain. Electromechanical or hydraulic devices are feasible actuator solutions, whereas the utilization of piezoelectric or magneto-resistive material integrated into the structure of the flexible leading edge was ruled out due to unsolved manufacturing, maintenance issues and power requirement [6].

As in SADE the enhanced adaptive droop nose was simply an extruded 2D wing section, within the SARISTU project it represents a 3D free-formed surface, which has to be smoothly modified between the shape for high-lift and cruise flight [7][8]. The objective is to develop a mechanical kinematic system with minimal deviation from optimal kinematical path in consideration of limited available design space, aerodynamic loads and manufacturing constrains. Taking into account the need of simultaneous and uniform deformation of all differently sized kinematic stations implies great effort in the design phase [9].

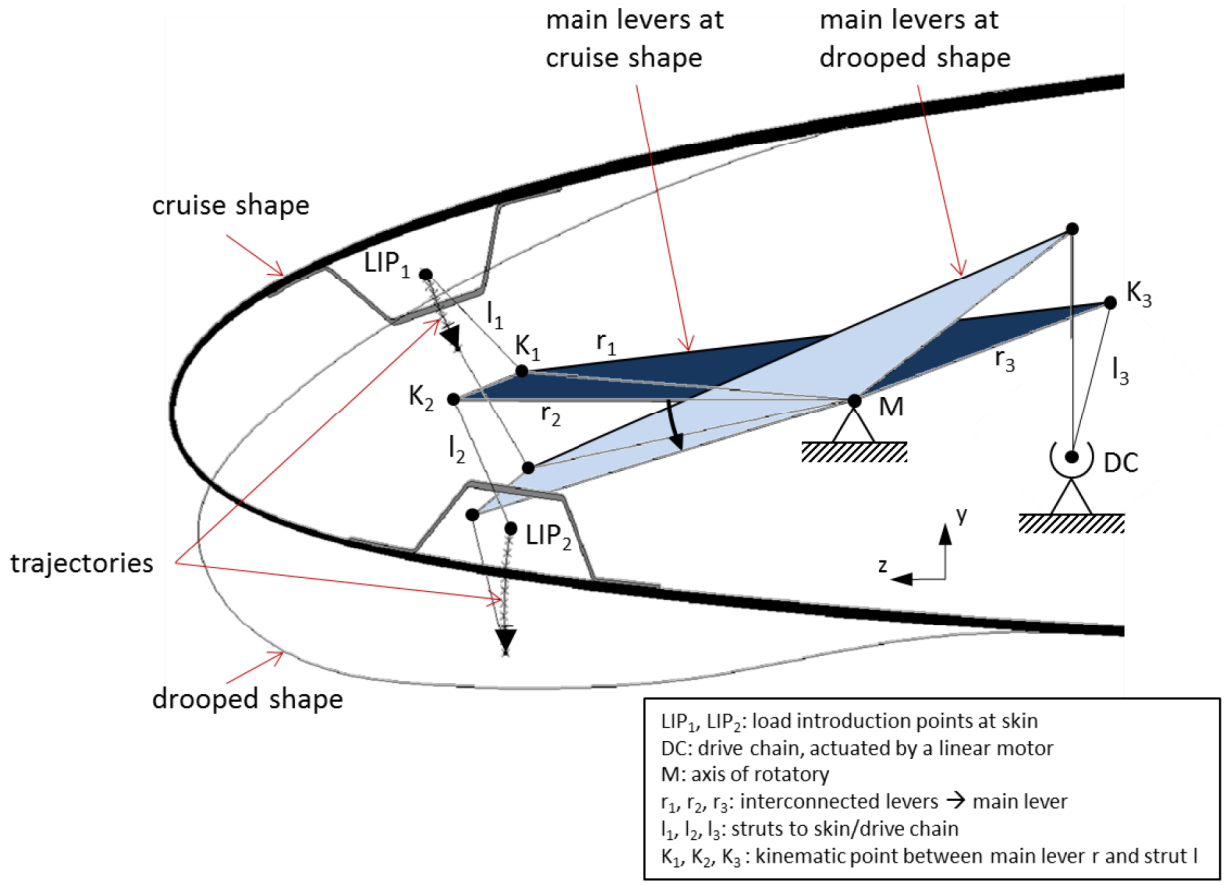

Figure 1: Cross-section of an enhanced adaptive droop nose with an integrated kinematic system for a morphing wing at cruise and (graying out) at drooped position

A separation of actuation and skin is mandatory to meet the joint aviation requirements [10]. The loads introduced by the skin are distributed at discrete support points along the span and in chordwise direction of the wing. The large deflection versus little space allocation

ratio removes the possibility for directly reaching the support points with the actuator which has the consequence that a new kinematic drive-chain is utilized, as depicted in Figure 1. This new kinematic drive-chain translates the linear motion of the main drive actuator into a synchronous, rotatory movement of a main lever. As the rotatory movement has to be synchronous for each spanwise kinematic station, consequently all main levers show the same axis of rotation and uniform kinematic connection to the drive actuator. Hence, the overall system fulfills the requirement of a least complex actuation system by firstly creating and secondly exploiting the advantage of synergies.

Regarding a single spanwise kinematic station, the main lever is in fact an interconnection of various individual lever. The main lever is linked on one side to the overall drive chain DC by using the strut l_3, whereas the spherical bearings of this strut allow an out of plane rotational movement. One huge benefit of this drive mechanism is that the actuator forces are remarkably minimized by supporting the introduced loads by means of the inner structure. This is the result of the varying gearing factor, determined by the angle between the cross link and the drive-chain. At drooped position a right angle between the cross link and drive chain is designed, which reduces the actuator forces theoretical to zero. On the other side the main lever is linked to the skin by using the struts l_1 and l_2, which are attached inside of the stringers at the skin brackets. The measure of locating the load introduction points LIP_1 and LIP_2 inside of the stringers increases the limited design space and, therefore, enables a better kinematic design (patent pending).

3 COMPUTATIONAL MODELING

3.1 NUMERICAL OPTIMIZATION

For optimization purposes the kinematic system is simplified to a reduced subsystem that consists of a single load introduction point K linked by a lever kinematics l and r with the actuation system DC. A crucial factor is the main lever, which ensures same rotational angle for all kinematic subsystems. Independent of its actuation the rotatory movement of the main lever is responsible for simultaneous and uniform deformation of the skin, which is predefined by the trajectories of the load introduction point (provided by project partner DLR). The mathematical formulation of the optimization problem uses the discrete-time positions of LIP-trajectories as the input parameter, the kinematic points K and M as independent variable and the rotational angle α as dependent output variable. As the structural conditions limit the position of the axis of rotation M to a small area and a large rotational angle α is desirable to achieve low bending moment, the position M and the angle α are given manually apriori. By this means, the inner optimization loop is considered to apply the quadratic deviation of the calculated rotational angle from the target rotational angle $(\alpha_{calculated} - \alpha_{target})^2$ as the optimization function is merely dependent on the position of the kinematic point K. A helpful secondary condition, to fulfill the requirement of simultaneous and uniform deformation of the skin, is given by the variances of all rotational angles at the same time step. The sum of the variances is added to the optimization function by a weighting factor. Depending on the weighting factor the result of the optimization can be focused on achieving small deviations between the different lever kinematics either at a special droop angle and/or at a certain range of droop angles. If the result of the inner optimization loop leads to undesirable results like length of struts too short, crossing struts or angle between skin and struts out of range (70°-110°), then the target rotational angle has to be adapted or even the axis of rotation M has to be changed.

In the literature this kind of lever kinematics is described as a crank mechanism with an

eccentrically mounted shaft [11]. The difference to the presented problem is that the offset q between the rotational axis M and motion direction p is so great that no complete rotation of the lever r is possible, as shown in Figure 2. Actually, only a pivoting motion is necessary to move the load introduction point from cruise position x_c to droop position x_d. The distance from the top dead center O_B to a random load introduction point B is described by the equation

$$x = \sqrt{(l+r)^2 - q^2} - l \cdot \cos\beta + r \cdot \cos\varphi \,. \tag{1}$$

Although the notation of this equation (1) is fairly simple, it is hardly possible to transform it in an appropriate form to solve the optimization problem. Another approach has to be taken for the numerical optimization.

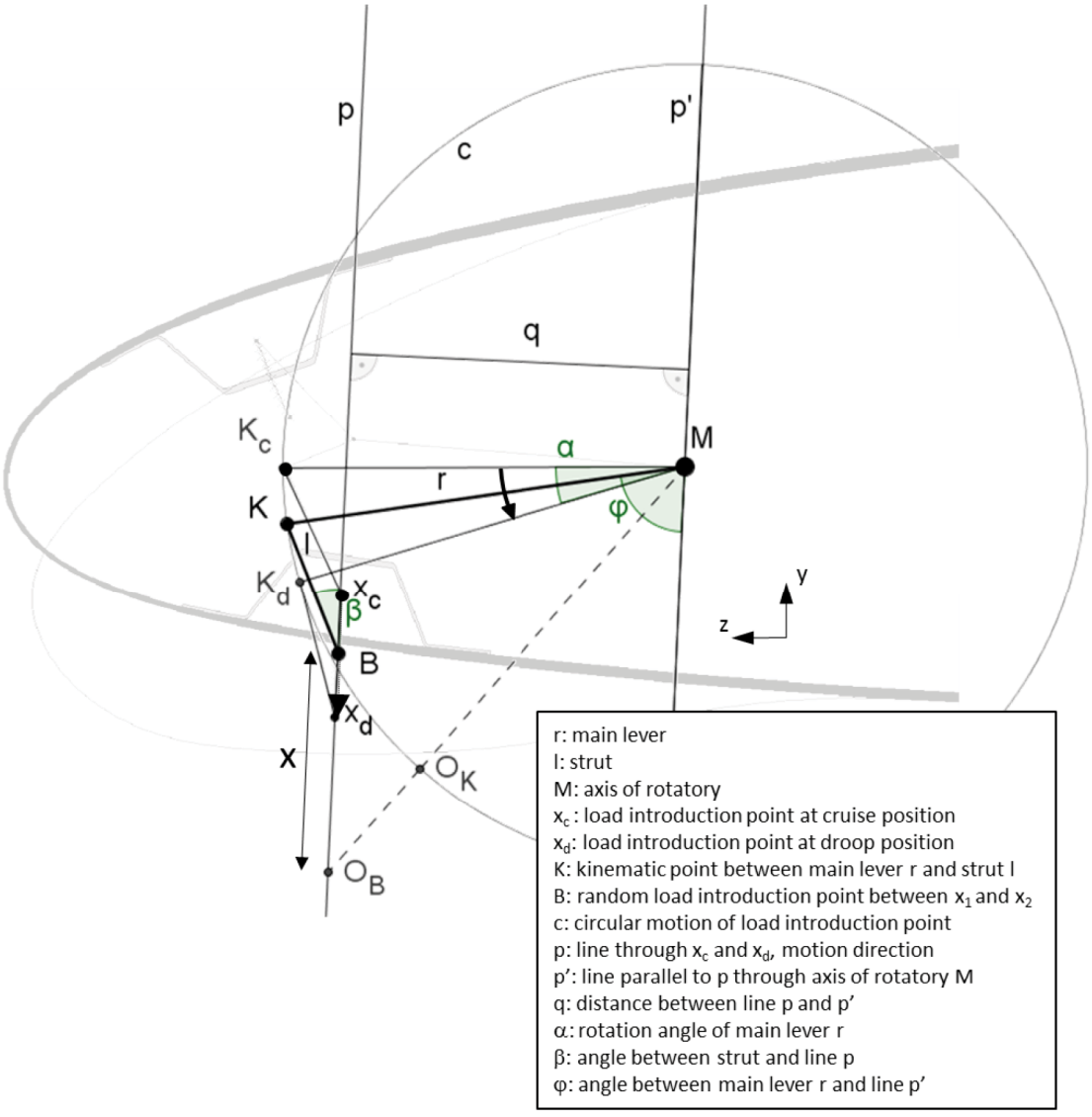

Figure 2: Simplification of the kinematic station by a crank mechanism with an eccentrically mounted shaft

The newly selected approach for the equation for the numerical optimization is established based on the law of cosines for arbitrary triangles. The equation calculates the rotational angle α by using the distance formula in the Cartesian coordinate system, it is described with

$$\alpha = \sigma - \varepsilon \text{ , or} \tag{2}$$

$$\alpha = \arccos\left(\frac{r^2 + b^2 - l^2}{2 \cdot r \cdot b}\right) - \arccos\left(\frac{r^2 + b^2 - w^2}{2 \cdot r \cdot b}\right), \text{ with}$$

$$r = \overline{K_c M} = r' \text{ , } l = \overline{K_c x_c} = l' \text{ , } b = \overline{x_d M} \text{ and } w = \overline{K_c x_d} \text{ .}$$

The improvement of this approach is, that the rotational angle α is directly derived by the kinematic points K_c and M for the given load introduction points at cruise position x_c and droop position x_d, as illustrated with Figure 3.

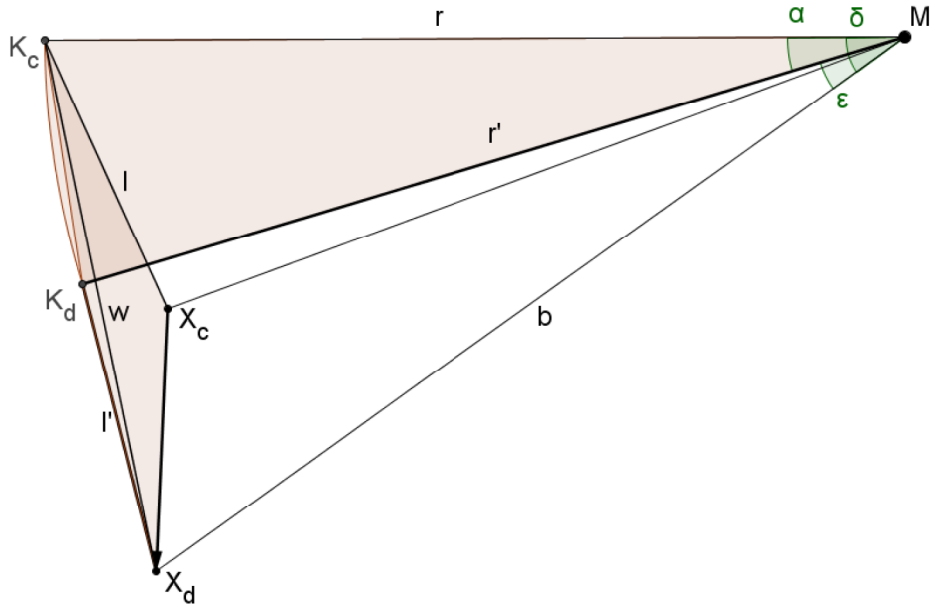

Figure 3: Geometrical description to the equation applied for the numerical optimization

The drawback of the presented numerical approaches is, that the kinematic point K_c could not be derived for a given rotational angle α and axis M. Especially the dependency of the rotational angle α would be very helpful, because in most cases the uniformity of motion can be verified by selecting three different points of the trajectories, e.g. cruise, drooped position and another position in-between. Furthermore the information of possible kinematic points K_c can immediately show, if generally a solution is possible and which measures are necessary to achieve a good solution.

3.2 GEOMETRICAL CONSTRUCTION METHOD

In contrast to the numerical approach, the geometrical construction method allow to visualize all valid kinematic points K_c, which result from inputs given by two load introduction points (e.g. at cruise position x_c and droop position x_d), rotational angle α and rotational axis M. This methodology (patent pending) enables not only to find a very precise kinematic solution in a convenient way, but also the impact of variation on each parameter becomes obvious and which measures for improvement can be taken. Likewise here, a reduced subsystem consisting of a single lever kinematics is used, that will be assembled to an overall system at the final stage. Geometrically the possible kinematic points K_c lie along a straight line. If the rotational axis M is fixed, which is usually the case, this line is

exclusively depending on the rotational angle α. As curves with equal angle dependency are also described as isogonic lines, this naming will be utilized for the line of possible kinematic points K_c.

One simple method to generate the isogonic line is illustrated in Figure 4 for the case, that the movement of all kinematic points is in-plane. The procedure is as follows, the end point (the load introduction point x_d) is rotated around the rotational axis M by the rotational angle -α to create the new point x_d'. The line segment bisector generated from the two points (1) the starting point (the load introduction point x_c) and (2) the new defined point x_d' characterizes the isogonic line Iso for the start position of all possible kinematic points K_c. The rotation of the line Iso around the rotational axis M by the rotational angle α leads to the isogonic line Iso' characterizing the end position of all possible kinematic points K_d. The idea behind this construction method is that the line segment bisector represents the set of all possible points between two reference points with the same distance to the reference points. This line segment bisector represents therefore the set of points, which have the same distance to the starting points and also to the by -α rotated end points. Points with the same distance to the start points and the by -α rotated end points represent instantaneously the possible kinematic points for this lever kinematics.

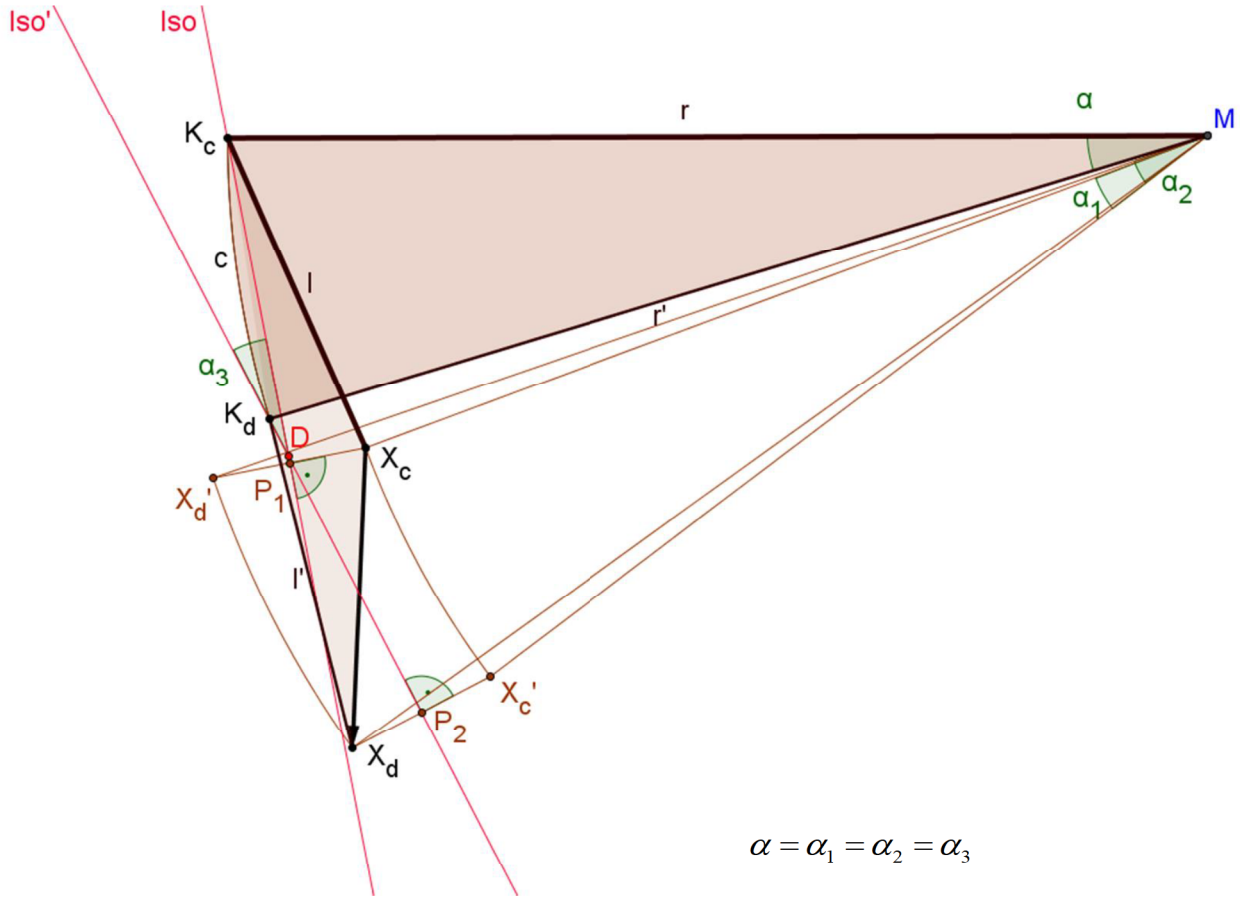

Figure 4: Graphical illustration of the design procedure for the isogonic lines in case of 2D movement

The isogonic line provides the information that inaccuracies in production along the isogonic line have no effect on reaching the end position by a given rotational angle α, but could lead to unequal deformation of the skin. On the other hand, orthographic deviations

from the isogonic line have huge impact on reaching the end position, depending how close together the isogonic lines of different rotational angles α are lying.

Even though the isogonic line represents all valid kinematic points K_c to move the load introduction point from start position x_c to end position x_d of the trajectory, the way of movement between these positions is not constantly progressing and, in fact, is dependent from the location of kinematic point K_c on the isogonic line. That's why for synchronization of all different lever kinematics it is favorable not to generate only a single isogonic line but also taking at least another position of the trajectory in-between. At a defined time step the corresponding positions on the trajectory can be taken as an intermediate end-position together with an adapted target rotational angle to generate the associated isogonic line. Crossing these isogonic lines indicates the optimum for the kinematic point K_c.

For deformation of the flexible skin of the SARISTU project there are 14 different-sized lever kinematics required; seven kinematic stations with two lever kinematics each. Its interconnection is achieved by same rotational angle of each main lever. With Figure 5 the cross-section of SARISTU airfoil with all lever kinematics is shown. The characteristic of nearly same slopes of isogonic lines are a sign for an overall good solution, regarding the upper and lower kinematic stations separately. The selected hinge points (K_c) are the result of crossing the isogonic lines with intersection lines. These intersectional lines are selected due to the fact, that they represent in average the best solution for simultaneous and uniform deformation. In addition it simplifies the construction of the kinematic. A subsequently numerical optimization process was deliberately not performed, because the resulting misalignment of the skin is already within the required tolerances.

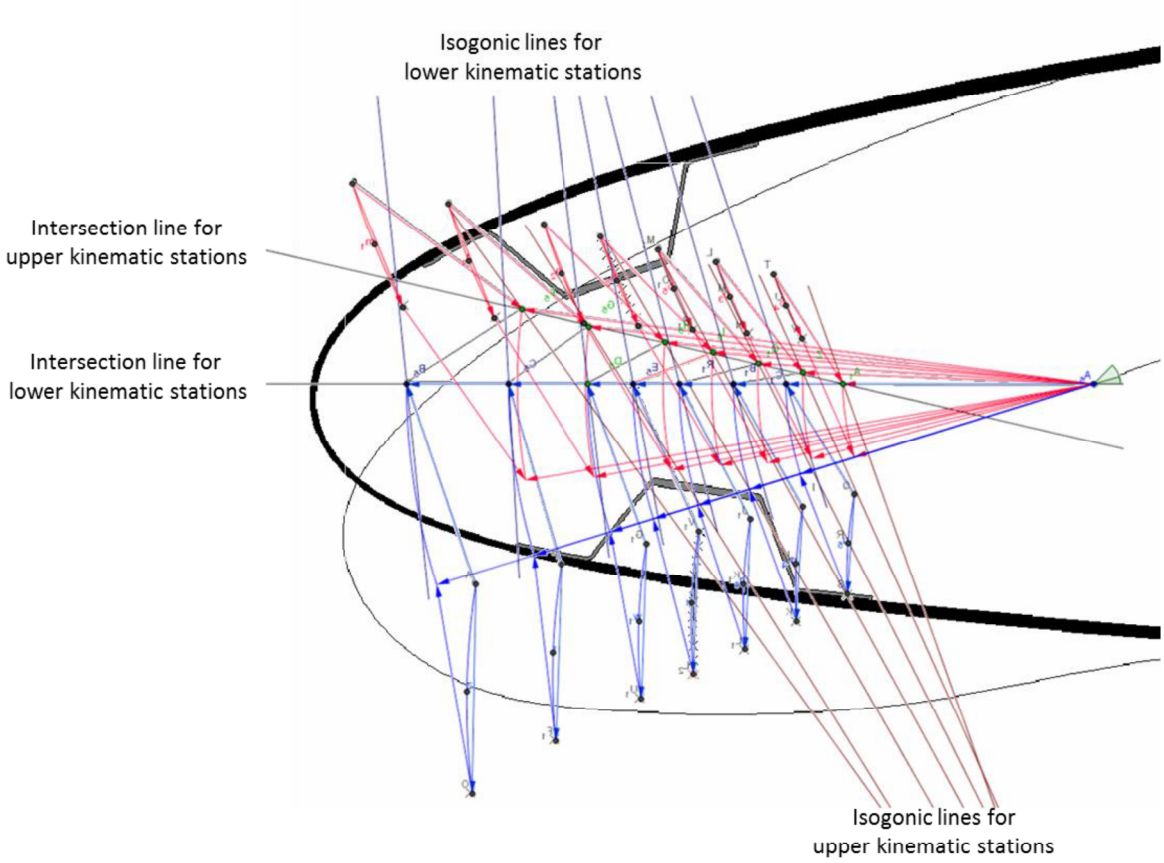

Figure 5: Cross-section of SARISTU airfoil with all lever kinematics together with the overlay of isogonic and intersection lines

Finally the main levers are linked to the overall drive chain DC using a similar lever kinematics, consisting of a main lever r and a strut l as described above. But the crucial difference is that the movement of the strut connected to the drive chain goes out-of-plane. Due to the fact that all main levers are synchronized by means of the same rotational axis and rotational angle, only one single design of cross link is required.

For an arbitrary arrangement of rotational movement and linked trajectories in a three-dimensional space it is still possible to construct an isogonic line. As shown in Figure 6, the linear motion of the drive-chain (form x_c to x_d) is parallel to the rotation axis of the main lever. For simplification purposes a coordinate transformation is carried out, whereby the rotational axis through M is equivalent to the z-coordinate axis. The methodology to generate the isogonic line is similar to the previous description for the two-dimensional case. Instead of the line segment bisector the bisecting plane is utilized. Afterwards, the intersection of the rotational plane (xy plane) with the bisecting plane results in the depicted isogonic line. Especially for the design of this lever kinematics, connecting the main lever with the drive chain, the isogonic line is helpful. Appropriate kinematic points can be found, which are located within the limited design space and require only low actuator forces.

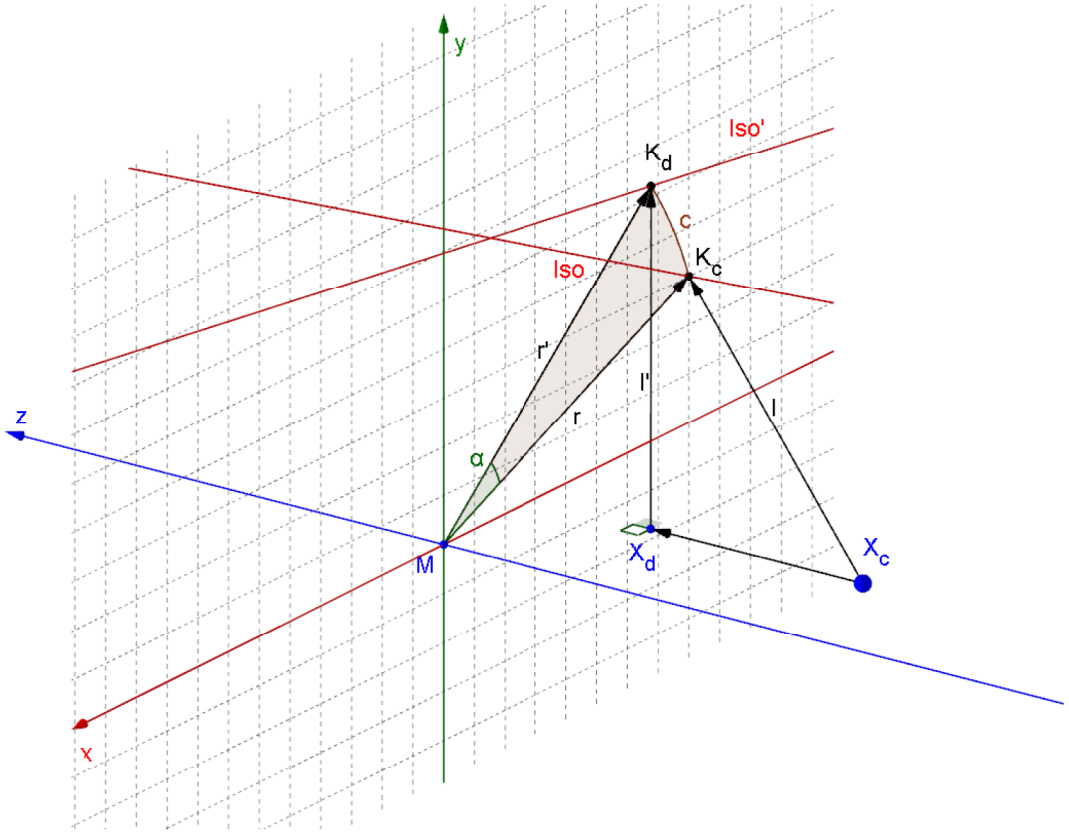

Figure 6: Graphical illustration for the usage of the isogonic lines to design a drive chain, general 3D construction method

The presented geometrical construction method can also be easily transferred to other application scenarios. The usage of this geometrical construction method is not only considerable for the development of actuation kinematics of a droop nose in future aircraft, but also for automotive, watercraft or even for wind power plants, whenever flexible, fluid-dynamic acting surfaces are employed [12].

9 CONCLUSIONS

The developed tool aims for minimal deviation from an optimal kinematical path and a simultaneous and uniform deformation of all differently sized kinematic stations. The methodology is split into a geometrical construction tool whose results go in a subsequent second numerical optimization tool. Design variables are hinge points and angles of the kinematics.

As presented at the conference we managed to design a droop nose suitable for a single aisle passenger aircraft. At the end of the project a full scale demonstrator will be tested in a wind tunnel under realistic flow conditions and a life-cycle ground test of the enhanced adaptive droop nose including bird strike will be performed, as shown in Figure 7.

In this study we are paving the way towards the industrial application of morphing wings in future aircraft.

Figure 7: Operation of the developed droop nose at the static test in the facilities of VZLU, Prague

ACKNOWLEDGMENTS

We would like to thank all participating partners from the FP7 project-consortium SARISTU for the good teamwork and the support during the development of the described kinematic system. Special thanks go to our partners DLR, INVENT GmbH and VZLU.

This work received funding from the European Union's Seventh Framework Program for research, technological development and demonstration under grant agreement no 284562.

REFERENCES

[1] SARISTU, FP7 project-consortium, http://www.saristu.eu
[2] ACARE, Vision 2020, European Commission
[3] ACARE, Flightpath 2050, European Commission
[4] Lorkowski, T.: Aktuatorsystem für "Morphing Devices" in SARISTU 1st Periodic Report Publishable Summary, SARISTU Consortium
[5] Hans Peter Monner, Markus Kintscher, Thomas Lorkowski, Stefan Storm: Design of a Smart Droop Nose as Leading Edge High Lift System for Transportation Aircraft, AIAA; 05/2009
[6] SADE Newsletter, 2012, SADE Consortium, www.sade-project.eu/publications.html
[7] Hochauftriebskonfigurationen, Invited Lecture, DLR Wissenschaftstag, Braunschweig, 30.09.2010
[8] Kintscher, M., Wiedemann, M., Monner, H.P., Heintze, O., Kuehn, T.: Design of a smart leading edge device for low speed wind tunnel tests in the European project SADE. International Journal of Structural Integrity, Vol. 2, No. 4, ISSN: 1757-9864, 2011.
[9] Monner, H. P., Riemenschneider, J. and Kintscher, M.: Groundtest of a Composite Smart Droop Nose. AIAA/ASMR/ASCE/AHS/ASC 2012, 23.-26.04.2012, Honolulu, Hawaii. ISBN 10.2514/6.2012-1580.
[10] Patent, Lift generating body for example an airfoil of adjustable variable cross-sectional shape, DE19792907912, Dornier Werke 1979
[11] K.-H. Grote und J. Feldhusen, Dubbel, Taschenbuch für den Maschinenbau, Springer Verlag, 23. Auflage, 2011
[12] Wolfgang Kempkens: http://www.ingenieur.de/Fachbereiche/Windenergie/Rotoren-Windraedern-passen-Form-blitzschnell-Wind-an